Theoretical study on the electronic spectrum of $[M(CN)_2]_n^{-n}$ (M = Au(I), Ag(I); n = 1–3) complexes

Fernando Mendizabal [a,*], Claudio Olea-Azar [b], Rodolfo Briones [b]

[a] Departamento de Química, Facultad de Ciencias, Universidad de Chile, Casilla 653, Santiago, Chile
[b] Departamento de Química Inorgánica y Analítica, Facultad de Ciencias Químicas y Farmacéuticas, Universidad de Chile, Casilla 233, Santiago 1, Chile

Abstract

The electronic structure and the spectroscopic properties of $[M(CN)_2]_n^{-n}$ (M = Au(I), Ag(I); n = 1–3) were studied using density functional theory (DFT) at the B3LYP level. The absorption spectrums in these complexes were calculated by single excitation time-dependent (TD) method. The di- and trinuclear models shown a $^1(n\mathrm{d}\sigma^* \rightarrow (n+1)\mathrm{p}\sigma)$ transition associated with a metal–metal charge transfer, which is strongly interrelated with the gold–gold and silver–silver contacts. The values obtained are in agreement with the experimental range.

Keywords: Gold(I); Silver(I); Electronic spectrum; TD-B3LYP

1. Introduction

Two of the typical metal that form compounds with the cyanide ion are the heavy metal ions Au(I) and Ag(I) [1]. The physical chemistry of gold(I) and silver(I) dicyanide complexes have been of considerable interests due to their importance in industrial applications [2–4]. The $[Au(CN)_2]^-$ and $[Ag(CN)_2]^-$ are representative linear two coordinate complexes thereby attracting much attention on the molecular and electronic structures.

Patterson and co-workers have shown that both $[Au(CN)_2]^-$ and $[Ag(CN)_2]^-$ ions undergo self-association in a variety of conditions, particularly in solutions [5–8]. Oligomerization of both ions is due to aurophilic Au–Au and argentophilic Ag–Ag interactions [9]. The aggregated forms are readily detected by their absorption and luminescent spectrums. Thus, the electronic spectra from solutions of $K[Au(CN)_2]$ and $K[Ag(CN)_2]$ varies from 180 to 450 nm depending upon the concentration. The experimental data are shown in Table 1 [5,6]. The absorption spectrums show a progressive red shifts with an increase in concentration. These results have been attributed to excited state interactions in oligomeric forms of these anions. Electronic structure calculations extended Hückel and MP2 suggest that this behavior is attributed to metal–metal interactions between neighboring $[Au(CN)_2]^-$ or $[Ag(CN)_2]^-$ ions [5–8].

The complexes studied here show evidence of metallophilic interactions. Closed-shell metallophilic interactions (d^{10}–d^{10}) are estimated to be energetically similar to hydrogen bonds (10–50 kJ/mol) [9,10]. At theoretical level, the attraction is estimated when electronic correlation effects are taken into account, strengthened by relativistic effects when the present heavy metals as the gold [11,12]. The mechanism behind such attraction is the dispersion (van der Waals) interaction, with additional allowance for virtual charge-transfer terms [13]. The optical properties of Ag(I) and Au(I) complexes have been calculated from CIS and higher levels [14,15]. Such properties have also been described efficiently through the Density Functional Theory (DFT) with the time-dependent (DFT-TD) approach, makes it the method of choice. Several works have shown an excellent association with experimental absorption and emission spectrums [16–20].

The objective of the present work is to study theoretically the excitation spectrums for systems of the type $[M(CN)_2]_n^{-n}$ (M = Au(I), Ag(I); n = 1–3) at B3LYP level. These systems could be used as models of the small oligimers responsible for electronic spectra observed from solutions of $K[Au(CN)_2]$ and $K[Ag(CN)_2]$. Thus far, no systematic DFT investigations have been carried out in models proposed.

* Corresponding author. Tel.: +56 2 978 7397; fax: +56 2 271 3888.
E-mail addresses: hagua@uchile.cl (F. Mendizabal), colea@uchile.cl (C. Olea-Azar).

Table 1
Experimental absorption spectra versus concentration of $K[Au(CN)_2]$ and $K[Ag(CN)_2]$ in aqueous solutions [5]

Concentration (M)	λ (nm)	Absorbance
$K[Au(CN)_2]$		
1×10^{-4}	196	1.3
	204	1.5
	219	1.3
	228	0.5
	236	0.4
1×10^{-2}	209	4.1
	228	4.4
	236	4.3
0.10	210	4.3
	233	4.8
	288	4.7
$K[Ag(CN)_2]$		
5×10^{-4}	199	1.1
1×10^{-3}	205	2.6
0.040	207	3.1
	223	2.6
0.30	206	3.6
	249	3.5
	278	2.9
0.80	208	4.1
	250	3.8
	279	3.2
	296	2.6

2. Models and methods

Models proposed $[M(CN)_2]_n^{-n}$ (M = Au(I), Ag(I); n = 1–3) used in our study are depicted in Fig. 1. The geometries were fully optimized to the indicated symmetry by the B3LYP method. Single point calculations of these geometries were simulating to study the excitation spectrums with TD-DFT. We have chosen for the models $[M(CN)_2]_2^{-2}$ (D_{2d}) and $[M(CN)_2]_3^{-3}$ (D_{2h}) the orientation staggered linear. This is due to the studied based on dimers of gold with orientation eclipsed show a strong repulsive term (quadrupole–quadrupole interaction) [21], while the models with staggered orientations are found to give a dispersive character in the metallophilic attraction.

Calculations using the GAUSSIAN 98 package were done [22]. The 19 valence-electron (VE) of Au and Ag quasi-relativistic (QR) pseudo-potential (PP) of Andrae [23] was employed. We used two f-type polarization functions on gold (α_f = 0.20, 1.19) and silver (α_f = 0.22, 1.72) [11]. Also, the atoms C and N were treated through PPs, using double-zeta basis sets with the addition of one d-type polarization function [24].

The energies excitation were obtained at the B3LYP level by using the time-dependent perturbation theory approach (TD-DFT) [25,26], which is based on random-phase approximation (RPA) method [27]. The TD-DFT approach provides an alternative to computationally demanding multi-reference configuration interaction methods in the study of excited-states. The TD-DFT calculations do not evaluate the spin–orbit splitting, the values are averaged.

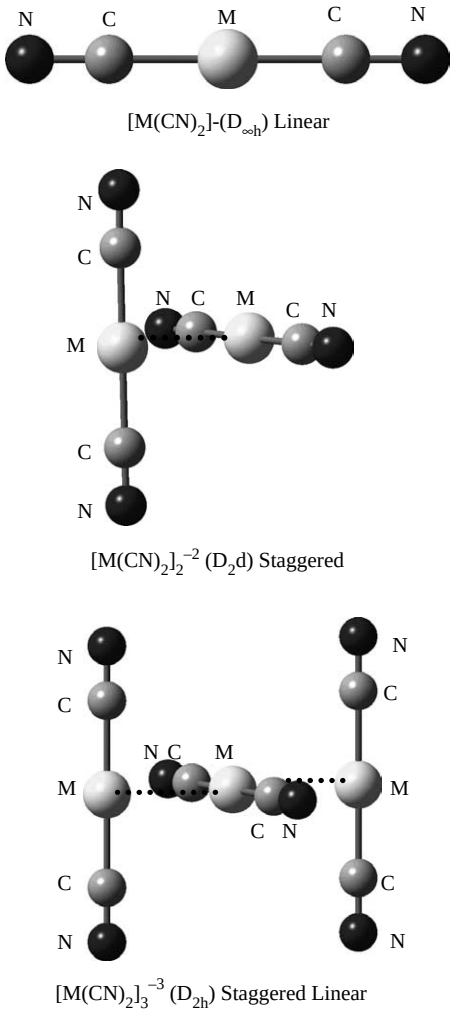

Fig. 1. Models: $[M(CN)_2]^-$, $[M(CN)_2]_2^{-2}$ and $[M(CN)_2]_3^{-3}$ (M = Au, Ag).

3. Results and discussion

3.1. Molecular geometry

Table 2 shows the main parameters of the models proposed. The theoretical results are in agreement with the experimental and theoretical data on the metal–metal contacts [28–31]. It is maintained in the experimental trend.

These results should be analyzed with caution, since DFT calculations using B3LYP do not describe rightly the metallophilic attraction; though DFT can reproduce the distance metallophilic [32,33]. The reason behind could be the specific form of the correlation energy, which it is not adequately described [11–13]. Moreover, the B3LYP functional is able to mimic the process near to the gold–gold and silver–silver equilibrium distance [29]. Our goal here is not to describe the metallophilic interaction and its magnitude, but the electronic spectrums for the systems mentioned.

Table 2
Main geometric parameters of the models (distances in pm and angles in degrees)

System	M–M	M–C	C–N	M–C–N (°)	Geometries
$[Au(CN)_2]^-$ $D_{\infty h}$ (**1**)		200.3	116.6	180.0	Linear
$[Au(CN)_2]_2^{-2}$ D_{2d} (**2**)	297.5	200.1	116.5	180.0	Staggered
$[Au(CN)_2]_3^{-3}$ D_{2h} (**3**)	303.4	200.1	116.4	180.0	Staggered linear
$[Ag(CN)_2]^-$ $D_{\infty h}$ (**4**)		205.2	116.7	180.0	Linear
$[Ag(CN)_2]_2^{-2}$ D_{2d} (**5**)	293.2	205.1	116.6	180.0	Staggered
$[Ag(CN)_2]_3^{-3}$ D_{2h} (**6**)	305.9	205.1	116.6	180.0	Staggered linear

3.2. Time-dependent (TD)-DFT calculations

We calculated the allowed spin singlet transition for the $[M(CN)_2]_n^{-n}$ (M = Au(I), Ag(I); n = 1–3) systems, based on the ground state structures of models **1**–**6**. The objective was to evaluate the electronic structure of the excited state by direct electronic excitations. Only singlet–singlet transitions were considered in these quasi-relativistic calculations. The allowed

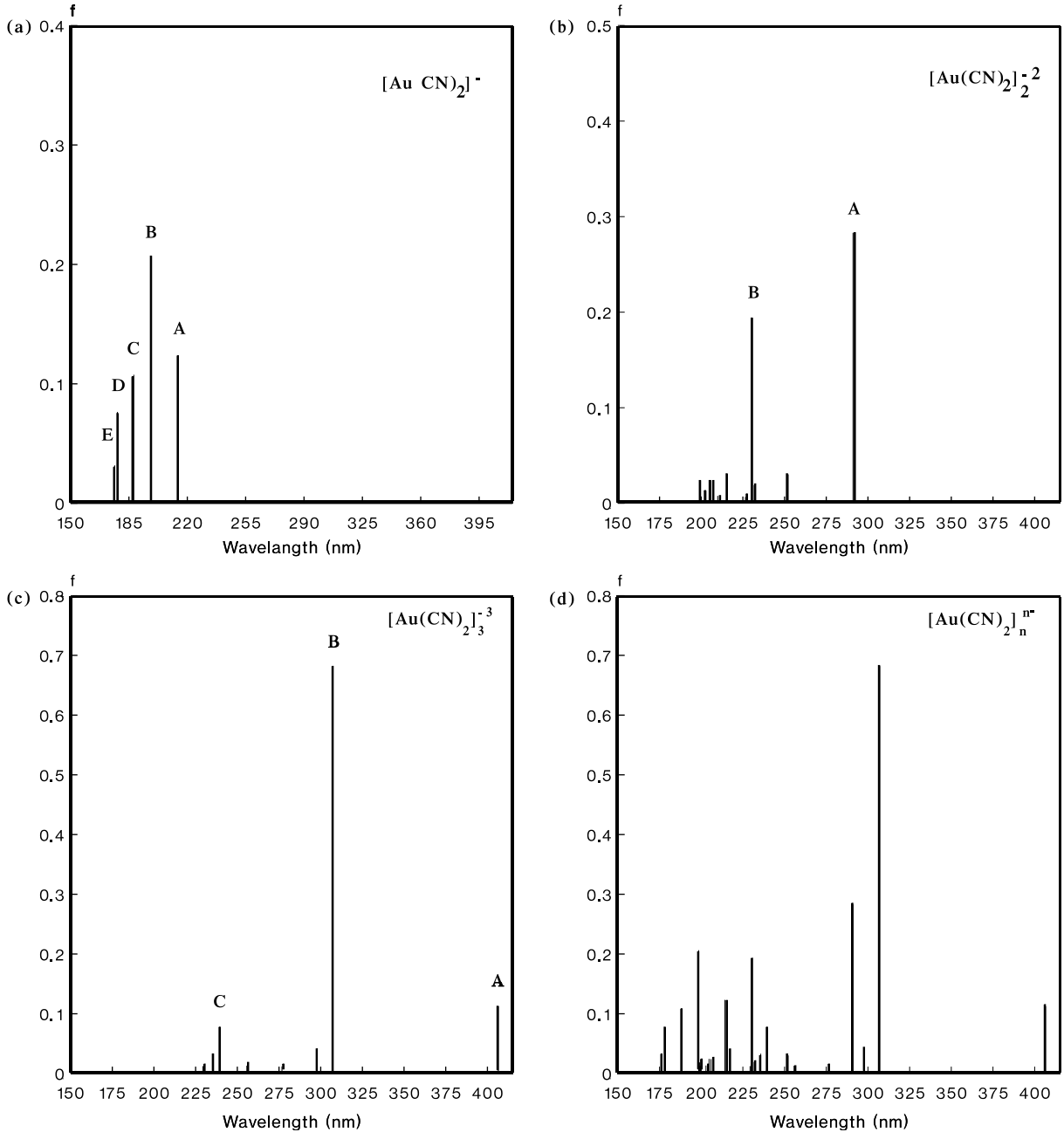

Fig. 2. The calculated electronic spectrums: (a) $[Au(CN)_2]^-$, (b) $[Au(CN)_2]_2^{-2}$, (c) $[Au(CN)_2]_3^{-3}$, (d) $[Au(CN)_2]_n^{-n}$.

transitions are shown in Figs. 2 and 3 and listed in Tables 3 and 4. Here, we consider as transitions permitted whose oscillator strength is different of zero. The molecular orbitals active the electronic transitions are proved in Figs. 4 and 5.

The experimental evidence shows that in dilute solutions (water and methanol) of $[Au(CN)_2]^-$ and $[Ag(CN)_2]^-$ ions are dominated by monomers; thus, metal–metal interactions are expected not to relevant in determining the electronic structure. The electronic structure of $[Au(CN)_2]^-$ and $[Ag(CN)_2]^-$ ions have been described with strong absorption bands in the ultraviolet range 250–180 and 195 nm, respectively, assigned to individual states of a metal-to-ligand charge transfer (MLCT) [5,6]. The absorption spectra in solutions of both ions show that increasing the concentration levels results in gradual increase in the relative intensity of the lower energy MLCT bands relative to the higher energy bands. On a concentration of 0.1 M solutions show a new shoulder in the 250–270 nm regions; this is transformed into new bands. As the concentration is progressively increased the absorption edge undergoes a corresponding red shift (see Table 1) [5–8]. Oligomerization of $[Au(CN)_2]^-$ and $[Ag(CN)_2]^-$ ions are clearly demonstrated. This indicates the presence of both $[M(CN)_2]^-$ monomer and $[M(CN)_2]_n^{-n}$ oligomer at higher concentrations.

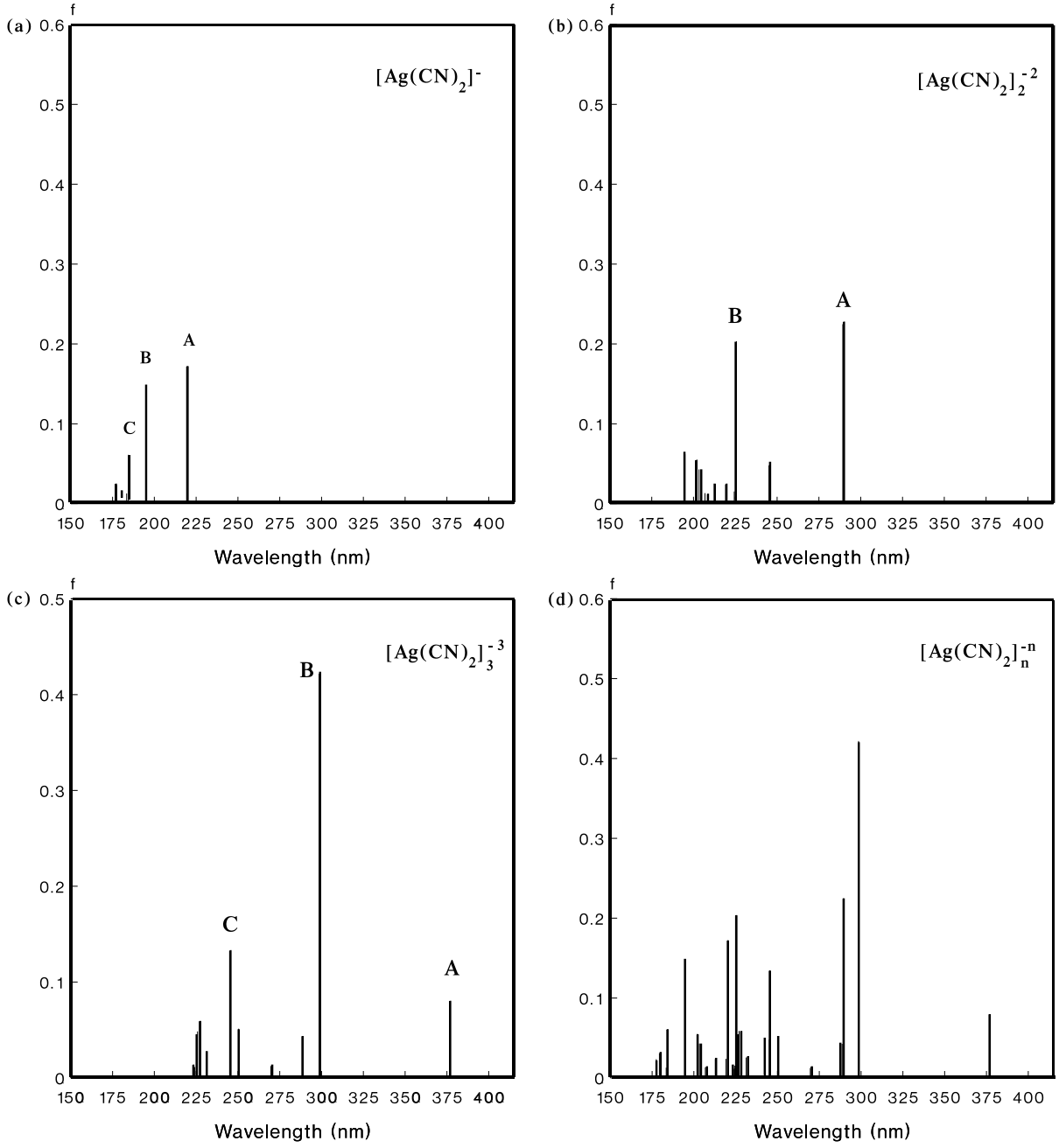

Fig. 3. The calculated electronic spectrums: (a) $[Ag(CN)_2]^-$, (b) $[Ag(CN)_2]_2^{-2}$, (c) $[Ag(CN)_2]_3^{-3}$, (d) $[Ag(CN)_2]_n^{-n}$.

Table 3
TD-DFT/B3LYP singlet-excitation calculations for $[Au(CN)_2]_n^{-n}$ ($n=1$–3)

Model	Excitation	λ_{calc} (nm)	f[a]	Contributions[b]	Type transition
$[Au(CN)_2]^-$ $D_{\infty h}$ (**1**)	A	214.2	0.1232	$14E_{2g}\rightarrow 21E_{1u}$ (4.50)	MLCT ($d_{xy}\rightarrow\pi^*$)
				$15E_{2g}\rightarrow 20E_{1u}$ (4.50)	MLCT ($d_{x2-y2}\rightarrow\pi^*$)
				$19A_{1g}\rightarrow 20E_{1u}$ (77.2)	MLCT ($d_{z2}\rightarrow\pi^*$)
				$19A_{1g}\rightarrow 21E_{1u}$ (8.30)	MLCT ($d_{z2}\rightarrow\pi^*$)
	B	198.5	0.2064	$17E_{1g}\rightarrow 20E_{1u}$ (42.3)	LLCT ($\pi\rightarrow\pi^*$)
				$18E_{1g}\rightarrow 21E_{1u}$ (42.3)	MLCT ($d_{xz}+\pi\rightarrow\pi^*$)
	C	187.9	0.1076	$14E_{2g}\rightarrow 20E_{1u}$ (8.60)	MLCT ($d_{xy}\rightarrow\pi^*$)
				$14E_{2g}\rightarrow 21E_{1u}$ (33.5)	MLCT ($d_{xy}\rightarrow\pi^*$)
				$15E_{2g}\rightarrow 20E_{1u}$ (33.4)	MLCT ($d_{x2-y2}\rightarrow\pi^*$)
				$15E_{2g}\rightarrow 21E_{1u}$ (8.60)	MLCT ($d_{x2-y2}\rightarrow\pi^*$)
				$19A_{1g}\rightarrow 20E_{1u}$ (6.50)	MLCT ($d_{z2}\rightarrow\pi^*$)
	D	178.1	0.0765	$12E_{1u}\rightarrow 22A_{1g}$ (82.1)	LMCT ($\pi\rightarrow$pz)
				$18E_{1g}\rightarrow 23A_{1u}$ (15.1)	MLCT ($d_{xz}+\pi\rightarrow\pi$)
	E	176.5	0.0318	$16A_{1u}\rightarrow 22A_{1g}$ (89.7)	MMCT ($d_{x2-y2}\rightarrow$pz)
				$19A_{1g}\rightarrow 23A_{1u}$ (7.60)	MMCT ($d_{z2}\rightarrow\pi$)
$[Au(CN)_2]_2^{-2}$ D_{2d} (**2**)	A	291.1	0.2831	$38B_2\rightarrow 40E$ (95.6)	MLCT ($d_{z2}+p^*\rightarrow\pi^*$)
	B	230.7	0.1940	$32B_2\rightarrow 40E$ (2.70)	MLCT ($p\rightarrow\pi^*$)
				$38B_2\rightarrow 43A_1$ (87.9)	MMCT ($d_{z2}+p^*\rightarrow s+p$)
$[Au(CN)_2]_3^{-3}$ D_{2h} (**3**)	A	406.6	0.1126	$57A_g\rightarrow 59B_{3u}$ (99.1)	MLCT ($d_{z2}+p^*\rightarrow\pi^*$)
	B	307.1	0.6821	$57A_g\rightarrow 60B_{3u}$ (89.9)	MMCT ($d_{z2}+p^*\rightarrow s+p$)
	C	239.5	0.0758	$43B_{3u}\rightarrow 58A_g$ (2.70)	MLCT ($d_{z2}+\pi\rightarrow\sigma_s^*$)
				$47A_g\rightarrow 59B_{3u}$ (13.4)	MLCT ($d_{z2}+d_{x2-y2}\rightarrow\pi^*$)
				$57A_g\rightarrow 66B_{3u}$ (77.8)	M CT ($d_{z2}+p^*\rightarrow\pi^*$)

[a] Oscillator strength.
[b] Values are $|coeff.|^2\times 100$.

3.2.1. $[Au(CN)_2]_n^{-n}$ ($n=1$–3)

The theoretical calculations are described in Table 3. The obtained spectrums are shown in Fig. 2(a)–(c). In Fig. 2(d), we have added the spectrums of the models **1**–**3** with the intention of appreciating the effect of all the systems simulating a high concentration in solution. There is a good agreement with the experimental bands.

For $[Au(CN)_2]^-$ $D_{\infty h}$ (**1**) model, we can observe that the theoretical excitations labeled A–E are related with the experimental spectrums described previously. The theoretical excitations match the experimental band (180–250 nm), when it is compared with a dilute solution (water and methanol) of $[Au(CN)_2]^-$ ion. The bands with greater contribution are mainly $19A_{1g}\rightarrow 20E_{1u}$ (77.2%, A), $18E_{1g}\rightarrow 21E_{1u}$ (42.3%, B),

Table 4
TD-DFT/B3LYP singlet-excitation calculations for $[Ag(CN)_2]_n^{-n}$ ($n=1$–3)

Model	Excitation	λ_{calc} (nm)	f[a]	Contributions[b]	Type transition
$[Ag(CN)_2]^-$ $D_{\infty h}$ (**4**)	A	220.2	0.1720	$19A_{1g}\rightarrow 20E_{1u}$ (35.8)	MLCT ($d_{z2}\rightarrow\pi^*$)
				$19A_{1g}\rightarrow 21E_{1u}$ (58.4)	MLCT ($d_{z2}\rightarrow\pi^*$)
	B	194.9	0.1470	$16A_{1u}\rightarrow 22A_{1u}$ (10.4)	MMCT ($d_{x2-y2}\rightarrow$pz)
				$17E_{1g}\rightarrow 20E_{1u}$ (40.4)	LLCT ($\pi\rightarrow\pi^*$)
				$18E_{1g}\rightarrow 21E_{1u}$ (40.4)	MLCT ($d_{yz}^*\rightarrow\pi^*$)
	C	184.4	0.0611	$14E_{1u}\rightarrow 22A_{1u}$ (31.0)	LLCT ($\pi\rightarrow\pi^*$)
				$15E_{1u}\rightarrow 22A_{1u}$ (59.8)	LLCT ($\pi\rightarrow\pi^*$)
$[Ag(CN)_2]_2^{-2}$ D_{2d} (**5**)	A	289.3	0.2247	$38B_2\rightarrow 40A_1$ (97.4)	MMCT ($d_{z2}+p^*\rightarrow\sigma$)
	B	225.7	0.2034	$37A_1\rightarrow 39B_2$ (33.7)	MMCT ($d_{z2}+p^*\rightarrow s^*$)
				$38B_2\rightarrow 44A_1$ (60.0)	MLCT ($d_{z2}+p^*\rightarrow\pi^*$)
$[Ag(CN)_2]_3^{-3}$ D_{2h}(**6**)	A	376.6	0.0793	$57A_g\rightarrow 58B_{3u}$ (98.9)	MMCT ($d_{z2}+p^*\rightarrow s+pz^*$)
	B	298.5	0.4219	$56B_{3u}\rightarrow 59A_g$ (3.40)	MMCT ($d_{z2}\rightarrow\sigma_s^*$)
				$57A_g\rightarrow 60B_{3u}$ (91.6)	MMCT ($d_{z2}+p^*\rightarrow pz^*$)
	C	245.8	0.1334	$53A_g\rightarrow 58B_{3u}$ (3.50)	MMCT ($d_{z2}\rightarrow\sigma^*$)
				$57A_g\rightarrow 65B_{3u}$ (89.7)	MLCT ($d_{z2}+p^*\rightarrow\pi^*$)

[a] Oscillator strength.
[b] Values are $|coeff.|^2\times 100$.

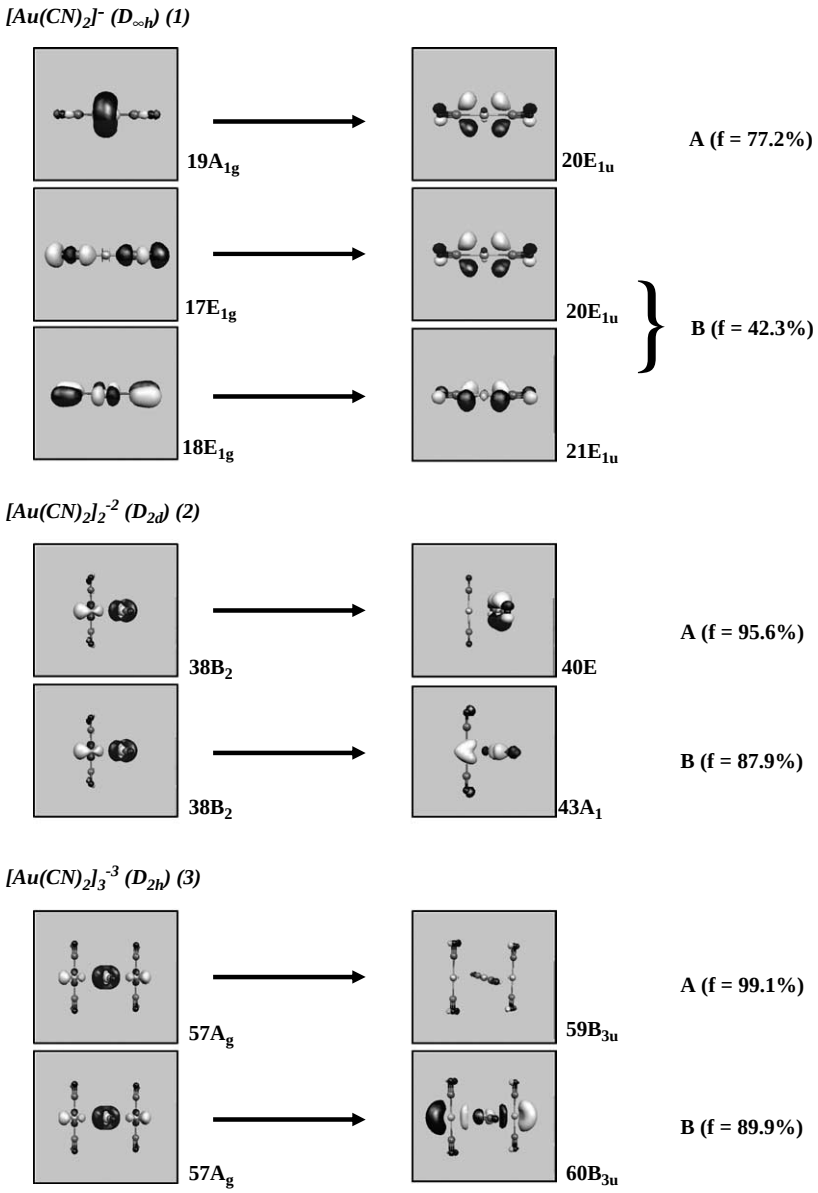

Fig. 4. The principal electronic transitions in the $[Ag(CN)_2]_n^{-n}$ ($n=1$–3) models.

$14E_{2g} \rightarrow 21E_{1u}$ (33.5%, C) and $12E_{1u} \rightarrow 22A_{1g}$ (82.1%, D). These bands correspond to metal-to-ligand charge transfer (MLCT). The E transition is associated to MMCT of energy higher $16A_{1u} \rightarrow 22A_{1g}$ (89.7%). The some molecular orbitals active involved in the electronic transitions are shown in Fig. 4.

When we use the models $[Au(CN)_2]_2^{-2}$ D_{2d} (**2**) and $[Au(CN)_2]_3^{-3}$ D_{2h} (**3**), we observe a red shift of the excited bands. The bands at higher wavelengths are mainly $38B_2 \rightarrow 40E$ (95.6%) and $57A_g \rightarrow 59B_{3u}$ (99.1%), predominantly involving a MLCT of type $d_{z2}+p^* \rightarrow \pi^*$, respectively. Furthermore, it appears a new transition (B) associate as metal-centered charge transfer (MMCT) $5d_{z2}(\sigma^*) \rightarrow 6p(\sigma)$, which we can understood from the O.Ms. shown in Fig. 4. This result shows that intermetallic interactions are mainly responsible for the new bands and demonstrated the presence of both $[Au(CN)_2]^-$ and $[Au(CN)_2]_n^{-n}$ ions.

3.2.2. $[Ag(CN)_2]_n^{-n}$ ($n=1$–3)

The results in the silver systems are very seemed to those of gold described in Section 2. The theoretical calculations are described in Table 4. The calculated spectrums are shown in Fig. 3(a)–(c). There is a good agreement with the experimental bands from different concentrations of solution of the $[Ag(CN)_2]^-$ ion [5].

For $[Ag(CN)_2]^-$ $D_{\infty h}$ (**4**), we can observe that the theoretical excitations labeled A–C are related with the experimental spectrum. The theoretical excitations match the experimental band (195 nm), when it is compared with dilute solution. They correspond to transitions of the type MLCT (A and B): $19A_{1g} \rightarrow 21E_{1u}$ (58.4%) and $18E_{1g} \rightarrow 21E_{1u}$ (40.4%), and LLCT (C): $15E_{1u} \rightarrow 22A_{1u}$ (59.8%).

When we use the models $[Ag(CN)_2]_2^{-2}$ D_{2d} (**5**) and $[Ag(CN)_2]_3^{-3}$ D_{2h} (**6**), we observe a red shift of the excited bands compared with the model $[Ag(CN)_2]^-$ $D_{\infty h}$ (**4**). In

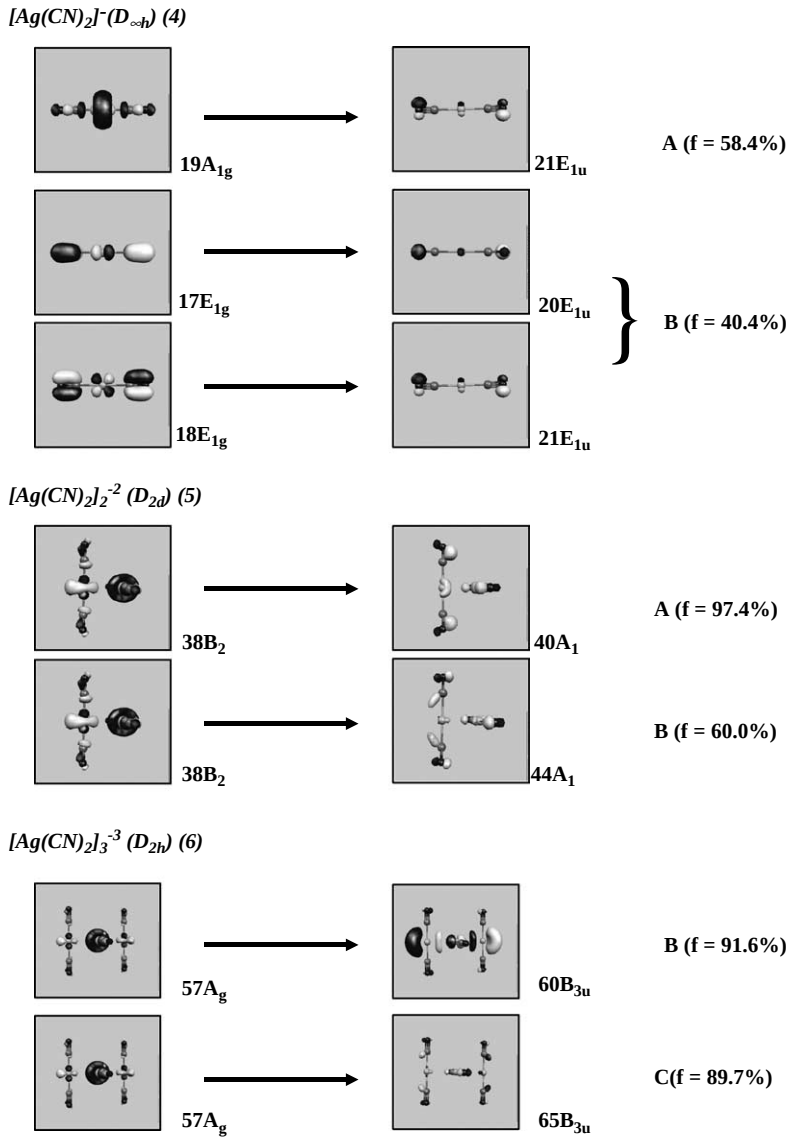

Fig. 5. The principal electronic transitions in the $[Ag(CN)_2]_n^{-n}$ ($n=1$–3) models.

both models (**5** and **6**), low energy bands (A and B) assigned to be the metal-centered charge transfer (MMCT) $4d_{z2}(\sigma^*)\rightarrow 5p(\sigma)$ (see Table 4 and Fig. 5). As in the gold models, it is explained through a red shift by the presence of the Ag–Ag contacts in the systems **5** and **6**. It is demonstrated in the presence of monomers and oligomers in the real solutions.

4. Conclusions

We have calculated electronic spectrums for the models **1**–**6** in the B3LYP version. The idea was demonstrated that is possible to describe such properties by the mono-, bi- and trinuclear gold(I) and silver(I) dicyanide complexes. TD-DFT calculations match the experimental excitation spectrums. They show that intermetallic interactions are mainly responsible by the $^1(nd_{z2}\sigma^*\rightarrow(n+1)p\sigma)$ MMCT. There is a strong dependency between the metal–metal contact in each system and the MMCT band, existing a effect of red shift that is evidence at experimental level.

Acknowledgements

This investigation was financed by FONDECYT no. 1020141 (Conicyt-Chile) and MIDEPLAN through Millennium Nucleus for Applied Quantum Mechanics and Computational Chemistry P02-004-F.

References

[1] A.G. Sharpe, The Chemistry of Cyano Complexes of the Transition Metals, Academic Press, London, 1976.
[2] Y.F. Jia, Q. Zhu, K.M. Thomas, Chem. Phys. Lett. 371 (2003) 105.
[3] F.S. Shan III, Chem. Rev. 99 (1999) 2589.
[4] F.E. Wagner, S. Haslbeck, L. Stievano, S. Calogero, Q.A. Pankhurst, K.-P. Martlinek, Nature (London) 407 (2000) 691.
[5] M.A. Rawashdeh-Omary, M.A. Omary, H.H. Patterson, J. Am. Chem. Soc. 122 (2000) 10371.

[6] M.A. Rawashdeh-Omary, M.A. Omary, H.H. Patterson, J.P. Fackler, J. Am. Chem. Soc. 123 (2001) 11237.
[7] M.A. Omary, H.H. Patterson, J. Am. Chem. Soc. 120 (1998) 7696.
[8] S.M. Kanan, C.P. Tripp, R.N. Austin, H.H. Patterson, J. Phys. Chem. B 105 (2001) 9441.
[9] P. Pyykkö, Chem. Rev. 97 (1997) 597.
[10] H. Schmidbaur, Gold Bull. 33 (2000) 1.
[11] P. Pyykkö, N. Runeberg, F. Mendizabal, Chem. Eur. J. 3 (1997) 1451.
[12] P. Pyykkö, F. Mendizabal, Inorg. Chem. 37 (1998) 3018.
[13] P. Pyykkö, Angew. Chem. Int., Ed. Engl. 41 (2002) 1001.
[14] H.-X. Zhang, C.-M. Che, Chem. Eur. J. 7 (2001) 4887.
[15] Q.-J. Pan, H.-X Zhang, Eur. J. Inorg. Chem. (2003) 4202.
[16] F. Mendizabal, C. Olea-Azar, Int. J. Quantum Chem. 103 (2005) 34.
[17] E.J. Fernández, M.C. Gimeno, A. Laguna, J.M. López-de-Luzuriaga, M. Monge, P. Pyykkö, D. Sundholm, J. Am. Chem. Soc. 122 (2000) 7287.
[18] V. Barone, F. Fabrizi de Biani, E. Ruiz, B. Sieklucka, J. Am. Chem. Soc. 123 (2001) 10742.
[19] E.J. Fernández, P.G. Jones, A. Laguna, J.M. López-de-Luzuriga, M. Monge, J. Pérez, M.E. Olmos, Inorg. Chem. 41 (2002) 1056.
[20] E.J. Fernández, A. Laguna, J.M. López-de-Luzuriaga, F. Mendizabal, M. Monge, M.E. Olmos, J. Pérez, J. Chem. Eur. J. 9 (2003) 456.
[21] P. Pyykkö, F. Mendizabal, Chem. Eur. J. 3 (1997) 1458.
[22] M.J. Frisch, G.W. Trucks, H.B. Schlegel, P.M.W. Gill, B.G. Johnson, M.A. Robb, J.R. Cheeseman, K.T. Keith, G.A. Petersson, J.A. Montgomery, K. Raghavachari, M.A. Al-Laham, V.G. Zakrzewski, J.V. Ortiz, J.B. Foresman, J. Cioslowski, B.B. Stefanov, A. Nanayakkara, M. Challacombe, C.Y. Peng, P.Y. Ayala, W. Chen, M.W. Wong, J.L. Andres, E.S. Replogle, R. Gomperts, R.L. Martin, D.J. Fox, J.S. Binkley, D.J. Defrees, J. Baker, J.P. Stewart, M. Head-Gordon, C. Gonzalez, J.A. Pople, GAUSSIAN 98, Rev. A.11, Inc., Pittsburgh, PA, 2002.
[23] D. Andrae, U. Häusserman, M. Dolg, H. Stoll, H. Preuss, Theor. Chim. Acta 77 (1990) 123.
[24] A. Bergner, M. Dolg, W. Küchle, H. Stoll, H. Preuss, Mol. Phys. 80 (1993) 1431.
[25] R. Bauernschmitt, R. Ahlrichs, Chem. Phys. Lett. 256 (1996) 454.
[26] M.E. Casida, C. Jamorski, K.C. Casida, D.R. Salahub, J. Chem. Phys. 108 (1998) 4439.
[27] L. Olsen, P. Jϕrgensen, in: D.R. Yarkony (Ed.), Modern Electronic Strucuture Theory, vol. 2, World Scientific, River Edge, NJ, 1995.
[28] J.C.F. Colis, R. Staples, C. Tripp, D. Labrecque, H. Patterson, J. Phys. B 109 (2005) 102.
[29] E. Colacio, F. Lloret, R. Kivekäs, J. Ruiz, J. Suárez-Varela, M.R. Sundberg, Chem. Commun. (2002) 592.
[30] J.C.F. Colis, C. Larochelle, E.F. Fernández, J.M. López-de-Luzuriaga, M. Monge, A. Laguna, C. Tripp, H. Patterson, J. Phys. Chem. B 109 (2005) 4317.
[31] M.-S. Liao, X. Lü, Q.-E. Zhang, Int. J. Quantum Chem. 67 (1998) 175.
[32] S.-G. Wang, W.H.E. Schwarz, J. Am. Chem. Soc. 126 (2004) 1266.
[33] E. O'Grady, N. Kaltsoyannis, Phys. Chem. Chem. Phys. 6 (2004) 680.